Eur. Phys. J. AP **3**, 159–167 (1998)

THE EUROPEAN PHYSICAL JOURNAL APPLIED PHYSICS

Characterization and realization of a 120 kV, 200 ns transmission line pulse generator

M. Rivaletto[a] and P. Pignolet

Laboratoire de Génie Électrique, Université de Pau, 64 000 Pau, France

Received: 17 December 1997 / Revised: 26 March 1998 / Accepted: 09 April 1998

Abstract. A 120 kV / 200 ns / 13 J transmission line generator building is accurately studied. A design method for achieving compact and reliable Blumlein generators is elaborated and validated by three realizations. In order to estimate the transmission line transformer amplification and droop, a set of equations is established and a new simplified gain expression is suggested. Another set of equations to characterize the secondary parasitic lines is settled. By turning it to account, an innovating building method using iron powder to reduce the transmission line transformer parasitic effects, is proposed. In this case, the transmission line generator energy yield reaches 93%.

PACS. 82.40.Mw Pulse techniques – 84.70.+p High-current and high-voltage technology: power systems; power transmission lines and cables (including superconducting cables)

1 Introduction

Some high pulsed power devices require for their applications, a MW peak pulse power, a reliable pulse wave shape, a minimum firing jitter, and a quite high repetition rate. Generally, in this case, the conventional pulse generators are not convenient because of their unreliability of pulse shape. So, it has been suggested to associate a low voltage pulse forming network achieving the required pulse shape and repetition rate, with a device which can give the desired voltage gain without any wave shape temporal degradation. The only method which seems capable of concillating all these requirements is the use of a Blumlein generator associated with a transmission line transformer. Although simple to build, the transmission line transformer displays a significant problem: parasitic lines or secondary lines which have a major effect upon its performance. Another problem comes from the load specifications which require a matching and a specific wave shape, namely a high voltage plateau duration (*i.e.* high power hyperfrequency tubes).

This paper deals with the development and the construction of a 120 kV / 200 ns / 200 Ω high voltage square pulse generator, based on the association of a 32 kV Blumlein generator with a four-stage transmission line transformer.

[a] e-mail: marc.rivaletto@univ-pau.fr

2 The Blumblein generator

2.1 The Blumlein generator principle

Various technologies are available for generating high voltage square pulses with a short rise time and a given width. One of these many solutions consists of using a Blumlein generator [1] which is convenient by dint of its simplicity, compactness and changeability.

The generator design principle [2] is based on two identical transmission lines, (1) and (2), supplied by a d.c. electrical source as shown in Figure 1. The device as a whole is put into action by firing a fast closing switch. This operation can be roughly described as follows: both lines are charged, through a high impedance R_{lim}, to the $V_H V$ initial d.c. voltage, the switch is closed at the initial time $t = 0$ and this launches a negative voltage pulse down the line (1). When the pulse reaches the termination, a time duration τ later, it increases and produces

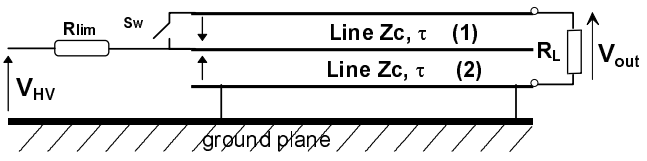

Fig. 1. Blumlein generator principle.

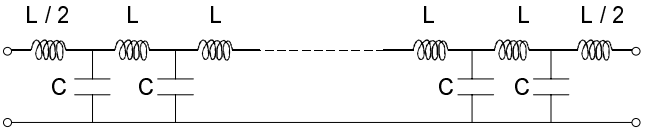

Fig. 2. Blumlein generator line principle.

through the load a voltage of magnitude:

$$V_{out} = \frac{2R_L}{R_L + 2Z_c} V_{HV}$$

where R_L and Z_c are respectively the load resistance and the transmission line characteristic impedance.

The output voltage stays on for a period 2τ, where τ corresponds to the transit time of each transmission line.

The rise time of the high voltage pulse is mainly determined by the closing time of the switch and the characteristic response time of one transmission line.

In the matched case when $R_L = 2Z_c$, the output voltage $V_{out}(t)$ is formed by a single pulse of voltage magnitude V_{HV} and with a duration $T_W = 2\tau$. On the contrary, when $R_L \gg Z_c$ this output voltage consists of multiple reflected pulses with a period 4τ and with a decreasing magnitude from the value $2V_{HV}$.

2.2 The Blumlein generator layout and construction

It is possible to use several technologies according to the operating voltage magnitude and the desired impedance: striplines, polymer insulated coaxial cables, liquid or gas insulated coaxial lines and discrete component associations. The last technology has been chosen because of its capability to form a compact set up and to operate at 50 kV. Furthermore the Blumlein generator described as follows has been built as a test device for the validation of the design method [3].

The corresponding schematic diagram is shown in Figure 2. The capacitors are discrete knob type H.V. ceramic components, the values of which range between 250 and 2 000 pF. On the contrary, the inductances are fully distributed along the transmission lines. However it is noticeable that an air inductance accurate value of about 50 nH is quite difficult to build. Furthermore, this value is similar to those of capacitor stray inductances. Consequently, this technique (air inductance) seems restricted to an output impedance $Z_{out} = 2\sqrt{L/C}$ much higher than 10 Ω.

However, an experimental investigation of a compact Blumlein generator will show the possibility of obtaining output impedance values much lower than 20 Ω with a sufficient pulse of about 200 ns.

2.3 The transmission line inductance

In the case of two conductive plates of width w, facing each other at a distance d, ($d \ll w$), if the plate thickness is neglected, the line inductance is commonly given by [4]:

$$L = \frac{4\pi \times 10^{-7} d}{w} \text{ [H]}. \quad (1)$$

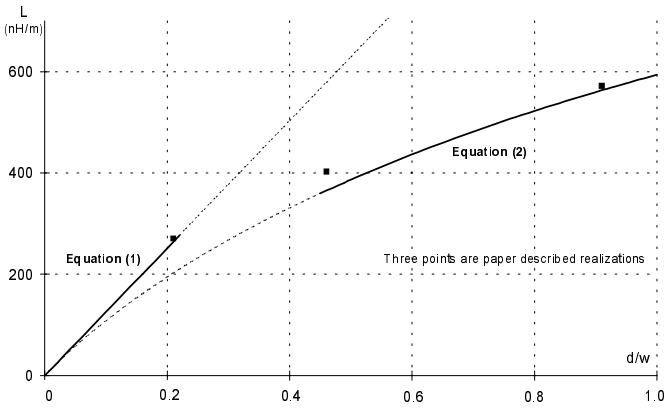

Fig. 3. Theoretical and measured inductance values *versus* d/w ratio.

However, in our limited space conditions, the device edges have to induce significant changes in the inductance value. So, by taking the edge effect into account, the equation (1) becomes [5]:

$$L = \frac{1\,183}{3 \times 10^8 \left[1 + \frac{\pi w}{d} + \ln\left(2\pi(\frac{w}{d} + 0.94)\right)\right]} \text{ [H]}. \quad (2)$$

Figure 3 shows a comparison between the theoretical and the measured inductance values for different ratios d/w. As can be seen, although the inductance values are not accurate when the values d/w are ranged between 0.3 and 0.4, by averaging the theoretical values deduced from both equations (1) and (2), a useful estimated one can be obtained and its accuracy can be better than ± 2 nH.

2.4 The design method

Usually, the main parameters of the Blumlein generator are: the maximum high voltage magnitude V_{HV}, the available pulse energy E, the output impedance R_L, and the pulse Full Width at Half Maximum (F.W.H.M.) T_w.

By introducing the number of elementary cells N_c in both lines, corresponding, in this peculiar case, to the number of capacitors, the capacitor C and the inductance L values, we get the following set of equations:

$$E = \frac{1}{2} N_c C V_{HV}^2$$
$$R_L = 2\sqrt{L/C}$$
$$T_w = N_c \sqrt{LC}\,.$$

Unfortunately, in this set of equations, V_{HV}, T_w, R_L, and E are not independent in the case of 100% efficiency:

$$E = \frac{V_{HV}^2}{R_L} T_w\,. \quad (3)$$

So, to solve this set of equations, V_{HV}, T_w, R_L being given, it is necessary to add another parameter. In practice the

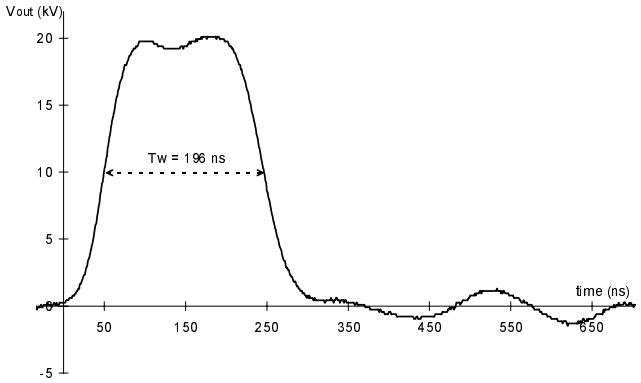

Fig. 4. Blumlein output voltage ($d/w \approx 0.21$; $L = 16$ nH; 3.3 Ω).

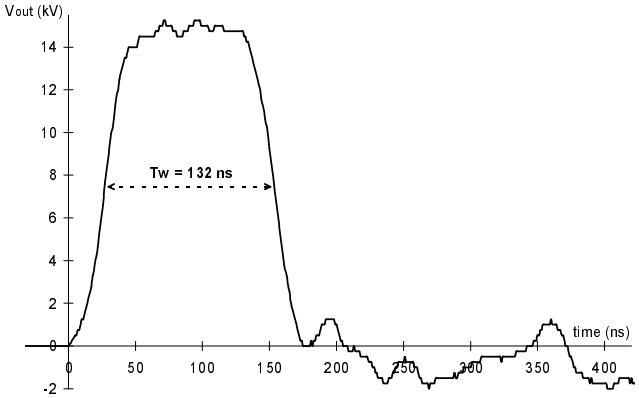

Fig. 5. Blumlein output voltage ($d/w \approx 0.48$; $L = 12$ nH; 12.5 Ω).

capacitor value is effectively given. Taking the assumption above into account, the solution in N_c and L can be written:

$$N_c = 2\frac{T_w}{R_L C}\ ;\ L = \frac{R_L^2 C}{4}\,.$$

Let us remark that N_c can be only an even natural number. Knowing the ceramic capacitor dimensions (diameter and height) and their number, the Blumlein generator dimensions are calculated from the equations (1) or (2). By keeping the same temporal characteristics, for a better compactness, the most convenient inductance expression will have to be chosen. When a lower impedance ($R_L < 5$ Ω) or a larger pulse F.W.H.M. are required, it is necessary to increase the number of capacitors and to connect them in parallel. In this case the previous method can be extended and the set of equations becomes:

$$\begin{aligned} E &= \frac{1}{2} N_c C V_{HV}^2 \\ R_L &= 2\sqrt{\frac{L}{N_l C}} \\ T_w &= 2N_L\sqrt{N_l L C} \\ N_c &= 2N_L N_l \end{aligned}$$

where N_l and N_L are respectively the number of identical capacitors for one cell and the number of cells for one transmission line. Obviously, the equation (3) always holds, and in addition to the previous parameters V_{HV}, T_w, R_L, and C, another parameter has to be given. If N_l is given, the solutions in N_c, N_L and L can be written:

$$N_c = 2\frac{T_w}{R_L C}\,;\ N_L = \frac{T_w}{R_L C N_l}\,;\ L = \frac{R_L^2 C N_l}{4}\,.$$

N_c and N_L are, respectively, an even natural number and a natural number. In this case, knowing the ceramic capacitor dimensions (diameter and height) and their number, because of the transversal arrangement of the capacitors, the Blumlein generator dimensions are generally deduced from equation (1).

Figures 4 and 5 show two examples of available wave shapes produced by two different Blumlein generators built according to the method above.

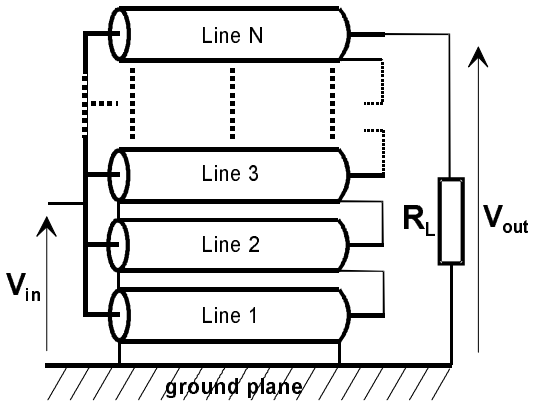

Fig. 6. Transmission line transformer principle.

3 The transmission line transformer

3.1 The transmission line transformer principle

The use of transmission lines to build up fast pulse transformers is well known in the pulsed power field [6–10]. Although its principle is simple, the transformer operation may appear surprisingly complicated because of the presence of secondary mode parasitic lines. The transmission line transformer principle can be explained from the N-stage transformer schematic diagram shown in Figure 6.

The setting up is composed of N identical cables connected in parallel at their input, and in series at their output. Each cable of characteristic impedance Z_c presents a propagation delay τ_d.

The input impedance of this cable arrangement is Z_c/N whereas the matched load is $Z_L = NZ_c$. So, when a square voltage pulse of magnitude V_{in} and F.W.H.M. τ_p is simultaneously applied to the N cable inputs, it propagates along each line. After a delay τ_d, the voltage pulse reaches the load termination. Since the line outputs are connected in series, the potentials of the inner conductor and the conducting braid of the cable i ($i = 1$ to N) are, respectively, theoretically raised to iV_{in} and $(i-1)V_{in}$ with respect to the ground. Consequently, in the case of a N stage transformer, the expected output voltage V_{out} is NV_{in}.

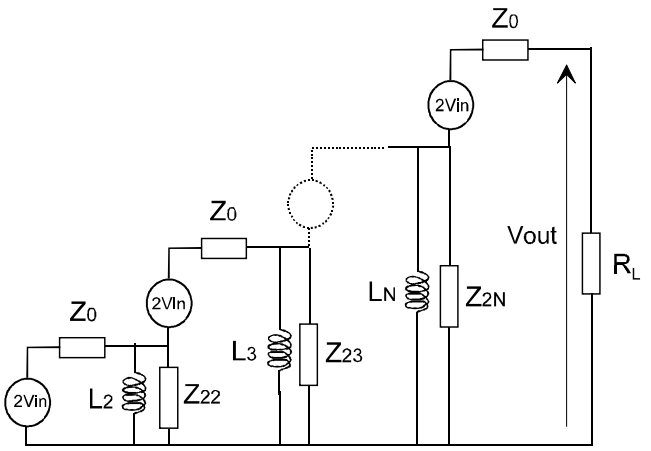

Fig. 7. N stage transmission line transformer equivalent scheme.

However, in the case of stacked lines, since the cable i ($i \neq 1$) is positioned on a straight line at the height h_i above the ground plane, a corresponding parasitic transmission line actually appears between its conductive braid and the ground. This is the so-called secondary mode line, the impedance of which is normally much greater than the cable characteristic impedance, and its propagation delay τ_{d_s} is less than τ_d. This secondary mode largely influences the expected voltage gain in the transient regime and the voltage droop in the permanent regime. For each cable i, $i \neq 1$, the secondary mode impedance can be considered as an additional impedance depending on the height [4]:

$$Z_{2i} = 138 \log\left(\frac{4h_i}{d}\right) \; ; \; h_i \gg d$$

where d is the corresponding cable braid outer diameter.

For a transformer maximum gain, the secondary mode impedance has to be as large as possible.

An equivalent schematic diagram of the N stage transmission line transformer is proposed in Figure 7 [8].

3.2 The general study

3.2.1 The pulse droop optimization

As it has been previously proposed by Wilson [7], for a weak droop ($< 10\%$), the inductance minimum value L_i for the transformer stage i can be written:

$$L_i = 10(i-1)Z_c T_w$$

where T_w corresponds to the pulse F.W.H.M.

Furthermore, by assuming that Z_{2i} are identical for each linear transmission line i, an analysis of the line transformer equivalent circuit, shown in Figure 7, leads to the following step response expression:

$$V_{out}(t) = \sum_{i=0}^{N-1} K_i \exp\left(-\frac{t}{\tau_i}\right) \text{ with } \tau_0^{-1} = 0\,. \qquad (4)$$

Empirically, the K_0 value and the number of terms increase with the number of the transformer stages. As the detailed expression becomes complicated when N is larger than 4, then N will be restricted to 4 .

In that case, the results of numerical simulations lead to the following remarks:

- As $Z_2 = Z_{2i}$ increases, the sum $\sum_{i=0}^{N-1} K_i$ increases independently of L_i. That means that the voltage gain $V_{out}(0)/V_{in}$ only depends on Z_2 for a given Z_c.
- The time constants τ_i are sufficiently different to consider one of them as predominant and affected by the largest one of the coefficients K_i. By assuming that K_{i-1} and τ_{i-1} are always respectively greater than K_i and τ_i, this condition is stated for $i = 1$. So, equation (4) can be written:

$$V_{out}(t) = K_0 + K_2 + K_3 + K_1 \exp\left(-\frac{t}{\tau_1}\right)\,. \qquad (5)$$

A sufficiently large value of τ_1 has to be chosen to make the pulse droop negligible. Consequently, the value of Z_2 has to be decreased. However, unfortunately, that is against the transformer's main properties: the amplification, which involves the secondary mode impedance, has to be as large as possible.

Consequently, a compromise consists of overestimating all the stage inductances by the value of the last stage one, so that:

$$L_i = L_N = 10(N-1)Z_c T_w\,.$$

By keeping the condition $T_w < \tau_1$ which generally holds, a linear approximation in equation (5) can be performed so that:

$$V_{out}(t) = \sum_{i=0}^{3} K_i - K_1 \frac{t}{\tau_1}\,.$$

As a summary, the time constant τ_1 which is involved in the pulse droop estimation can be finally written:

$$\tau_1 = \frac{L_N}{(N-1)Z_c} \text{ with } Z_2 = Z_{2i} \gg Z_c\,.$$

3.2.2 The secondary mode line removal

For the secondary mode impedance reduction, several methods are proposed in the literature such as [4,8,11]:

- To make a winding arrangement close to that of the U.H.F. choke coil with large distances between each turn. All of which is confined in a shielding.
- To consider a coaxial geometry where the cables are kept in a straight position and confined in a grounded coaxial socket.
- To make a winding arrangement with only one turn row uniformly wound with an helical form round an insulated cylinder. All of which is confined in a coaxial socket.

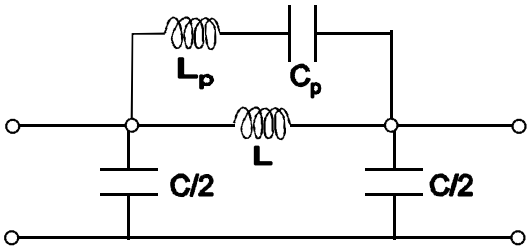

Fig. 8. Secondary mode line: one turn equivalent scheme.

- To make a winding arrangement with only one turn row uniformly wound with an helical form round a magnetic material core with a large magnetic permeability. The active conductors are away from the ground plane.

Although the last option presents some difficulties (saturation induced into the magnetic core by high current intensities), we will choose it.

So, in this simple case, the secondary mode impedance can be estimated straight from the following formula, based on the RG-65 cable conception method [12]:

$$L = \frac{4\pi^2 \mu_r n^2 r_L^2 \times 10^{-7}}{l} \quad [\mathrm{H}] \tag{6}$$

$$C = \frac{24 \times 10^{-12} l}{\log(2h/r_c)} \quad [\mathrm{F}] \tag{7}$$

$$Z_2 = \frac{129\pi n r_L}{l}\sqrt{\mu_r \log(2h/r_c)} \quad [\Omega] \tag{8}$$

$$\tau_{d_s} = 3.1\pi n r_L \sqrt{\frac{\mu_r}{\log(2h/r_c)}} \times 10^{-9} \quad [\mathrm{s}]\,.$$

where L, C, Z_2 and τ_{d_s} are respectively the coil inductance, the equivalent coil capacitor with respect to the ground plane, the secondary mode impedance and the corresponding propagation delay, and where: l is the coil length, r_L is the mean radius of the coil, r_c is the outer radius of the coil, n is the number of the coil turns, h corresponds to the distance between the outer part of the coil and the ground plane, μ_r is the relative magnetic permeability of the magnetic core.

Unfortunately, the previous results are no longer valid for all the frequencies. In particular, at high frequency, the stray capacitors located between the coil turns tend to decrease the secondary mode impedance and its corresponding delay. Consequently, the previous model will be valid solely for below megahertz frequencies.

Nevertheless a schematic bloc-diagram can be proposed as shown in Figure 8, where L and C are the previous inductance and capacitor values deduced from equations (6) and (7). L_p and C_p correspond to the equivalent stray inductance and capacitance [3].

Note that, in these conditions, the signal components, the frequencies of which are lower than $1/2\pi\sqrt{LC_p}$, ranged from 1 to 10 MHz, will "see" a high impedance (a few thousands ohms) formed by L and C_p and their corresponding delay will be long (100 ns/m). On the contrary, the signal components corresponding to the pulse rise edge, the frequencies of which are higher than 50 MHz, will "see" a weak impedance (a few hundred ohms formed by L_p and C) and their delay will range between 3 to 5 ns/m. That will involve a decrease in voltage gain and an increase in rise time. In order to avoid this, solutions, such as spacing the coil turns or spreading the cables in straight line and surrounding them by a magnetic material, can be considered.

3.2.3 The general voltage gain expression

By using the equivalent circuit shown in Figure 9, it is possible to deduce a general expression for the voltage gain (Gg) which enables an evaluation of the best construction technology [2,13].

So, by writing the Kirchoff's current law at the node K, the following voltage recursive relation can be written:

$$V_{K+1} - V_K\left(2 + \frac{Z_c}{Z_2}\right) + V_{K-1} = 0\,;\ K = 1 \text{ to } N-1\,. \tag{9}$$

By basing on the typical general solution $V_n = \lambda r^n$ and by introducing it into the equation above, a characteristic equation is obtained as follows:

$$r^2 - \left(2 + \frac{1}{a}\right) r + 1 = 0 \text{ where } a = Z_2/Z_c\,.$$

This equation has reciprocal roots (r_1 and r_2) which can be expressed as:

$$r_1 = \frac{1}{r_2} = \frac{2a + 1 - \sqrt{4a+1}}{2a}\,.$$

In the following demonstration, we chose to use the root which is less than 1 (*i.e.* r_1) because r_1^n tends towards 0 when n tends towards infinity (this property will be used to establish the Gg^∞ expression). The solution of the recursive equation (9) is now:

$$V_n = K_1 r_1^n + K_2 r_1^{-n}\,.$$

By using the boundary conditions in the case of a matched transformer:

$$V_0 = 0 \text{ and } V_N = \frac{(V_{N-1} + 2V_{in})N}{N+1}$$

and by choosing a solution like:

$$V_n = K(r_1^n - r_1^{-n}) \text{ with } K = K_1 = -K_2$$

the solution for the nth transformer stage is:

$$V_n = \frac{2r_1 n(r_1^{2n} - 1)V_{in}}{(n+1)r_1^{n+1} - nr_1^{2n} - (n+1)r_1 + nr_1^2}\,.$$

So the general expression of the voltage gain for an N stage transmission line transformer can be written as follows:

$$Gg^{(N)} = \frac{V_{out}}{V_{in}} = \frac{V_N}{V_{in}} = \frac{2N(1 - r_1^{2N})}{(N+1)(1 - r_1^{2N}) + Nr_1(r_1^{2N-2} - 1)}\cdot \tag{10}$$

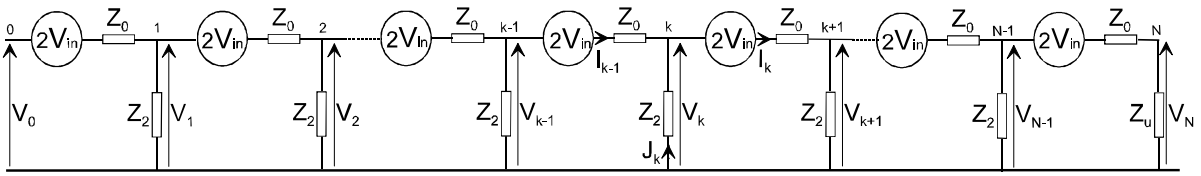

Fig. 9. Voltage gain calculation: T.L.T. equivalent scheme.

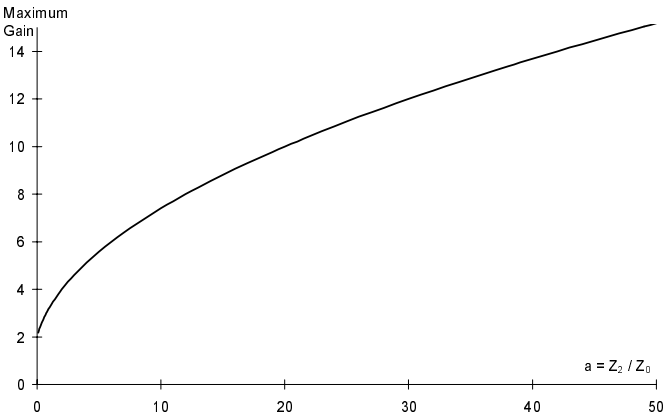

Fig. 10. Theoretical Gg^{∞} *versus* Z_2/Z_0 ratio.

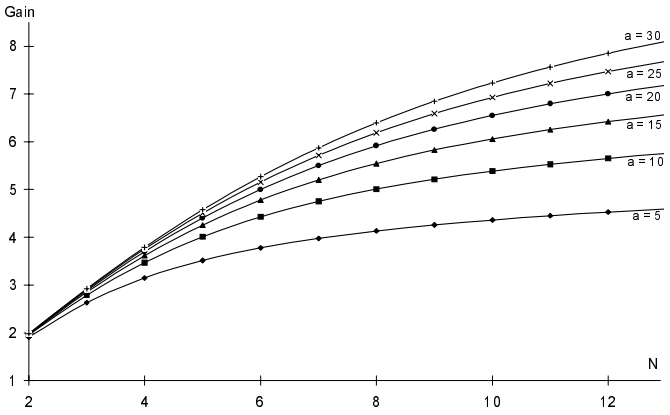

Fig. 11. Theoretical $Gg^{(N)}$ *versus* N for some ratios $a = Z_2/Z_0$.

Note that when N tends towards infinity the gain $Gg^{(N)}$ becomes:

$$Gg^{\infty} = \frac{4a}{\sqrt{4a+1}-1}\,.$$

The gains Gg^{∞} and $Gg^{(N)}$ are presented respectively in Figure 10 and Figure 11 as a function of a and N for different values of a.

For standard values of $a = Z_2/Z_c$, $z = 1/a$ can be neglected with regards to the unity. So, by substituting r by $1-\sqrt{z}$ in equation (10), a simplified but novel expression of the gain G_S can be derived:

$$G_S = N - \frac{1}{2}\left(\frac{N^3}{3} - \frac{N^2}{2} + \frac{N}{6}\right) z$$

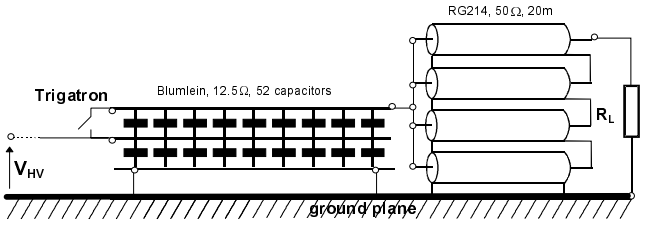

Fig. 12. Transmission line generator principle.

and, since

$$(\frac{N^3}{3} - \frac{N^2}{2} + \frac{N}{6}) = \sum_{i=1}^{N-1} i^2\,,$$

we can reduce this expression such as:

$$G_S = N - \frac{1}{2}\sum_{i=1}^{N-1} i^2 z\,. \qquad (11)$$

Note that the different approximations greatly depend on the number of stages and also on the value of z. For the validity of equation (11), the larger N will be, the more reduced z will have to be. In that case, relation (11) enables a first approach to the TLT design, thanks to a faster estimation of the component values (Z_c, N) and of the winding technology (Z_2).

Under these conditions, this relation (11) is in accordance with Mesyats and Chodorow results [13].

4 The high voltage pulse generator construction

Our technological aim is to build a 120 kV / 200 ns / 200 Ω high voltage pulse generator. Thus, according to the previous theoretical study, a 4 stage transmission line transformer connected to a 32 kV / 12.5 Ω Blumlein generator is considered. The complete generator layout is presented in Figure 12. For the 200 Ω output impedance, the most suitable technology is to use four 50 Ω coaxial cables. That involves a 12.5 Ω transformer input impedance.

4.1 The Blumlein generator construction and tests

By taking the generator compactness and a voltage hold off overestimation into account, the Blumlein generator has to be constructed with 2 nF knob type ceramic capacitors.

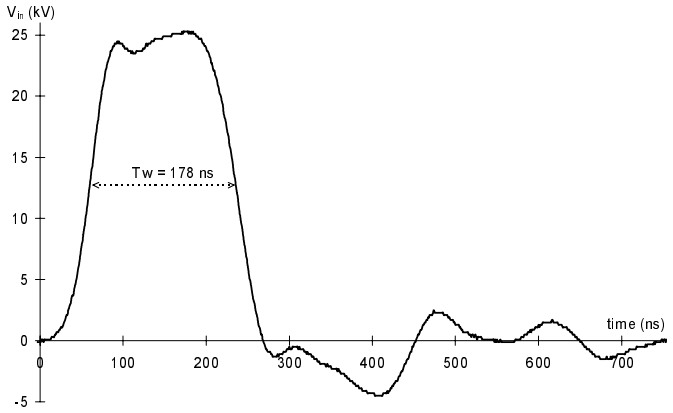

Fig. 13. Blumlein output pulse ($d/w \approx 0.91$; $L = 41$ nH; 12.5 Ω.

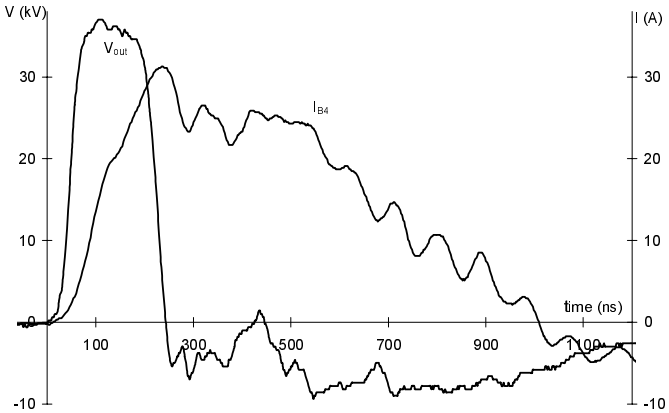

Fig. 14. Output pulse and fourth cable braid current shapes.

Thus, the 12.5 Ω impedance and the pulse F.W.H.M. ranging between 150 ns and 200 ns suggests the consideration of a cell number N ranging from 11 to 13, with a cell inductance of 41 nH and a cell capacitance of 1 nF. That leads to connect in series two capacitors of 2.1 nF to achieve a 1.05 nF cell capacitance. That conduces to use 44 or 52 capacitors of 2.1 nF. However, as the capacitor thickness is 3.2 cm, the plate spacing will be $d = 6.4$ cm. By taking this distance into account, equation (1) gives an overwidth $w = 30$ cm with a 180 cm overlength. That is not convenient. So, farther on, equation (2) will be considered.

The mechanical connections between the Blumlein generator and the transmission line transformer implicate the use of a plate width of 7 cm which corresponds to a ratio $d/w = 0.91$ and to an inductance of 563 nH/m. For a 41 nH cell inductance, that leads to adjust to 73 mm the space between each capacitor and a 100 cm overlength.

So, Figure 13 shows the high voltage output pulse generated by a 13 cell Blumlein generator (52 capacitors) supplied by a 25 kV d.c. high voltage.

All the voltage measurements are made with a PVM5 NORTHSTAR high voltage probe with a large frequency band or a capacitive divider probe. As it can be seen, the pulse F.W.H.M. of 178 ns agrees well with the model predictions. The energy available in the pulse's square shape corresponds to 9 J. By taking the design into account, one can expect to supply the Blumlein generator by a 80 kV d.c. voltage, which enables extending the output pulse energy to 90 J. As it can be observed in Figure 13, some reflections appear: this is due to the weak mismatching at both generator ends and at different connections, yet without damage to the useful part of the high voltage square pulse.

4.2 The transmission line transformer construction

The transmission line transformer is built with four 20 m / 50 Ω coaxial cables RG214-KX13. The corresponding inductance value of each cable in straight line position is 20 μH. The cable type and length choices have been laid down in connection with the following points:

- Due to the breakdown surface flashovers taking place at the cable end, it is necessary to remove the braid to a distance of 20 cm. Consequently, the cable d.c. voltage withstand is 100 kV.
- The cable droop is 0.024 dB/m for 10 MHz, and 0.11 dB for 200 MHz. So, as the rise time of the Blumlein generator output pulse is roughly 45 ns, the droop is much lower than 5%. A 5% droop value would be obtained for a 30 ns rise time signal.
- As for the secondary mode removal and a large pulse F.W.H.M. acceptance ($T_w > 100$ ns), it is necessary to consider a cable about 20 m long, in order to limit the voltage droop.

The four cables are wound round 12 cm outer diameter PVC tubes, forming now four 64 μH coils composed by 48 joined turns uniformly distributed along 55 cm. The lines (1) and (2) are placed 20 cm above the ground plane, whereas the lines (3) and (4) are placed 40 cm. The corresponding air capacitors measured with regards to the ground at 1 kHz are respectively 16 pF and 10 pF. That is in good agreement with the respective theoretical values computed from equation (7), namely 17 pF and 12 pF.

Figure 14 shows the braid current measured with a Pearson probe placed around the fourth cable on the transformer input side, and the output pulse, under a V_{HV} reduced value (10 kV).

In order to suppress the secondary mode, it has been necessary to increase the secondary mode inductances. Thus, a magnetic core has been made by filling a toroidal PVC tube with a F75 magnetic iron powder [14]. However, when it is pressed and fired at high temperature, this material has a magnetic permeability of 75, whereas in the powder form, its magnetic permeability is only 4.4.

The lines (3) and (4) are wound, as shown in Figure 15, round this magnetic core whereas line (2) is only wound round a PVC cylinder filled with the magnetic powder, so that the respective line inductance values become $L_2 = 205$ μH and $L_3 = L_4 = 280$ μH. The secondary mode modified currents, in the braids of the second and fourth cables, are presented in Figure 16.

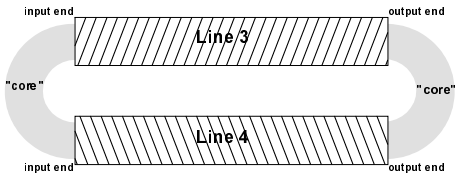

Fig. 15. Winding diagram of the TLT lines 3 and 4 (*idem* lines 1 and 2).

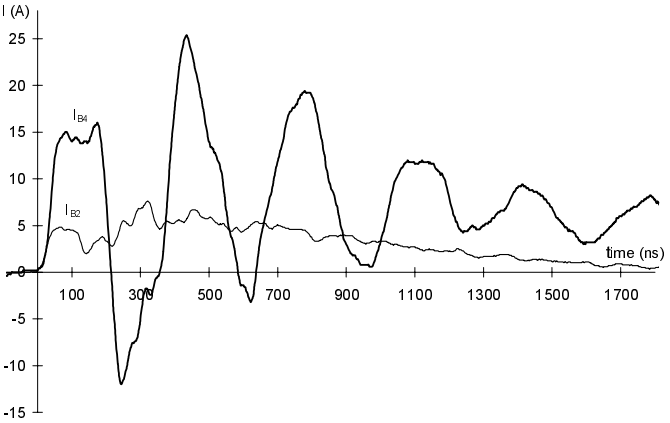

Fig. 16. Second and fourth cable braid current shapes.

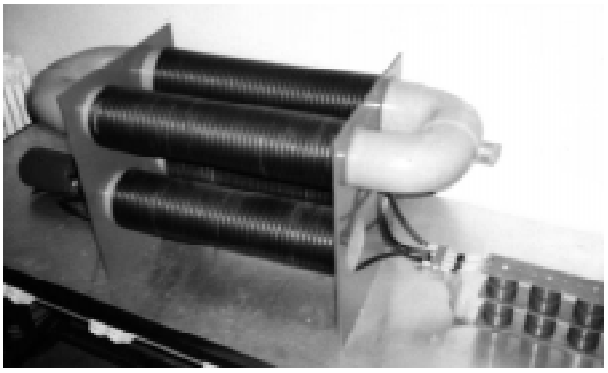

Fig. 17. Complete generator assembly (exploded view).

Figure 17 shows an exploded view of the complete generator assembly. The Blumlein generator appears on the right side, the load on the left side.

The input and output voltages are compared in Figure 18. The input voltage and output voltage measurements are performed, respectively with the previous high voltage probe, and the fast high voltage capacitive divider.

The comparison shows that the general temporal characteristics of the input and output pulses are well preserved, namely the rise time (46 ns and 47 ns) and the F.W.H.M. (178 ns and 180 ns).

The experimental voltage gain is roughly 3.75 which corresponds to a voltage yield of 93.8%. The pulse energy available is 13 J which has to be compared with the 14 J initially stored in the capacitors. That corresponds to an energy yield of 93%.

However, a degradation of the plateau is observed. That can be attributed to the actual frequency behaviour

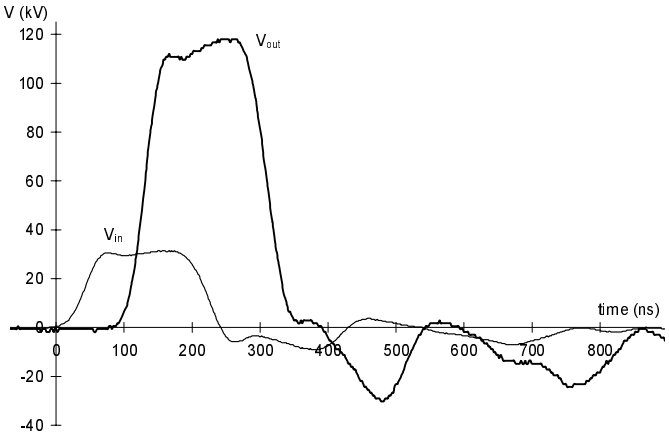

Fig. 18. Generator input and output pulses.

of the secondary mode impedance which is not easy to know. Moreover the secondary line is not completely homogeneous along its whole length, particularly at the connection ends. These corresponding inductances tend to reduce the secondary mode impedance.

In these conditions equation (8) gives a secondary mode impedance value of $Z_2 = 5\,000\ \Omega$. For this value, equation (11) gives a voltage gain of 3.9. However, the theoretical value of the secondary mode impedance which could correspond to the experimental voltage gain of 3.75, would be $1\,250\ \Omega$. Nevertheless, the difference between the theoretical and experimental voltage gains is lower than 5%.

5 Conclusion

As the weak pulse droop produced by high voltage generators is of great interest for the supply of hyperfrequency tubes, the study of a high voltage square pulse generator, based on the association of a Blumlein generator and a transmission line transformer, has been proposed.

Particularly, the main aspect of this work has been to elaborate a simple method to design such a generator by taking the compactness into account. So, the importance of the minimization of the Blumlein generator inductances leads to straightforward considerations about the generator dimensions.

It has been demonstrated that an hybrid technology, namely discrete components for capacitances and sheets for distributed inductances, can be simply modelled.

In the case of the transmission line transformer, the secondary mode, which occurs because of transient short circuit, is analysed. The partial removal of this involves the increase in the inductive part of the secondary mode impedance. A solution has been proposed by winding coaxial cables round a magnetic core.

This test device has been built in order to validate our design model. Considering the encouraging results and by using the same design model, we expect to reach soon 500 kV.

References

1. A.D. Blumlein, British Patent N° 589 127 (October 1947).
2. M. Kristiansen *et al.*, in *Pulsed Power short Course*, University course, Texas Tech. University, Lubbock, Texas.
3. M. Rivaletto, *Conception de générateurs de fortes puissances pulsées: mise en forme et caractérisation de l'impulsion haute tension*, Ph.D. thesis, Université de Pau, 1997.
4. J-P. Vabre, *Électronique des impulsions*, Tome 6, fascicule 2 (Éditions Masson, 1972).
5. P. Grivet, *Physique des lignes de HF et UHF*, Tome 1 (Éditions Masson, 1969), p. 143.
6. C.R. Wilson, P.W. Smith, *Transmission line transformers for high voltage pulsed power generation*, Proc. 17th Power Modulator Symposium (Seattle, 1986), p. 281–285.
7. C.R. Wilson, *The design and development of fast pulsed power supplies using transmission line transformers*, Ph.D. thesis, University of St Andrews, 1992.
8. I.A.D. Lewis, Electron. Engineering **27**, 448–450 (1955).
9. J.O. Rossi, P.W. Smith, *An analysis of the performance of linear transmission line transformers*, IEE Colloquium, Pulsed Power 97 (London, 19 March 1997).
10. P.N. Graneau *et al.*, Rev. Sci. Instrum. **67**, 2630–2635 (1996).
11. I.A.D. Lewis, F.H. Wells, *Millimicrosecond pulse techniques* (Pergamon Press LTD, London, 1954, new edition 1959).
12. H.E. Kallmann, *Proceedings of the I.R.E. and Waves and Electrons*, N° 34 (June 1946), p. 348–351.
13. A.M. Chodorow, *Proceedings of the IEEE* (July 1975), p. 1082–1084.
14. Groupe SAGEM, *Ferrite - Poudre de Fer - Fer Carbonyl* (Catalogue PF1, Société SAGEM, Paris, Juillet 1993).